

Supporting information for

PO(CH₂CH₂CF₃)₃: an Organic Ultraviolet Nonlinear Optical Material without any anionic group

Liting Lin^a, Xiaoqian Li^a, Kun Qian^{a,*}, Lin Cheng^a, Youquan Zhong^a, Hua Xu^b

^a College of Pharmacy, Jiangxi University of Traditional Chinese Medicine, Nanchang, 330004, P. R. China

^b International Education College, Jiangxi University of Traditional Chinese Medicine, Nanchang, 330004, P. R. China

Email: qk0876@hotmail.com

Synthesis

All the experimental instruments used in the reaction process were dried and wax seal was carried out at the interface of the experimental device because of the strict waterlessness required in the preparation of the Grignard reagent. A solution of POCl₃ (7.06 g, 0.046 mol) in 10 mL of anhydrous ether was added by drops to a Grignard reagent produced from CF₃CH₂CH₂Cl (19.6 g, 0.148 mol) and magnesium (6.20 g, 0.26 mol) in 100 mL of ether. The reaction mixture was heated for 4 h, cooled and treated with water, and then with a diluted HCl solution. The precipitate was filtered off, washed with water, dried in air, and recrystallized from a hot acetonitrile. PO(CH₂CH₂CF₃)₃ was formed as the fine needle-shaped crystals with a yield of 3.90 g (25 %), mp 193-195°C.

Single Crystal X-ray Diffraction

Single crystal X-ray data of compound **1** was gathered with MoK_α radiation ($\lambda = 0.71073 \text{ \AA}$) and CuK_α radiation ($\lambda = 0.15406 \text{ \AA}$) at 296(2) and 363.15 K respectively by using an φ - ω scan mode from a Bruker Smart APEX II diffractometer. We used the Crystal Clear software package (Rigaku, 2005) to complete data processing. We applied the SADABS program for absorption corrections. The SHELXTL program was used to determine the crystal structures and was used to refine by full matrix least-squares techniques. Table S1 presents the crystallographic information and the structural refinement data of compound **1** at different temperature. Table S2 - S3 present key bond distances and angles of compound **1** at different

temperature, respectively. Table S7 and Table S8 present anisotropic displacement parameters for compound **1** at different temperature, respectively.

Infrared spectroscopy

The infrared spectroscopy (IR) spectrum of compound **1** was obtained on a PerkinElmer infrared spectrometer in the range from 400 to 4000 cm^{-1} (see Fig. S1).

Thermogravimetry-mass Analysis

The thermogravimetry-mass (TG-MS) analysis for compound **1** was carried out with a PerkinElmer Exstar/TG6300 simultaneous analyser instrument. Crystal sample (5 ~15 mg) were enclosed in Al_2O_3 crucibles and heated from 30°C to 300°C at a heating rate of 10°C·min⁻¹ under a constant flow of nitrogen gas (see Fig. S5).

UV-vis Transmittance Spectroscopy

The UV-vis transmittance of compound **1** was measured on a PerkinElmer Lamda - 950 UV/vis/NIR spectrophotometer scanning in the range of 200 - 800 nm at room temperature with an unpolished crystal sample.

UV-Vis-NIR diffuse reflectance

The ultraviolet-visible-near-infrared (UV-Vis-NIR) diffuse reflectance spectrum of compound **1** was measured on a PerkinElmer Lamda - 950 UV/Vis/NIR spectrophotometer in the range of 200 - 700 nm at room temperature. And BaSO_4 was considered as the standard of 100% reflectance.

Second Harmonic Generation

Powder SHG signals were measured on Q-switched Nd: YAG laser at $\lambda = 1064$ nm fundamental wave laser radiations by using the Kurtz-Perry powder SHG technique.

Powder X-ray Diffraction

X-ray diffraction patterns of polycrystalline materials were obtained on a Dandong 3500 X-ray diffractometer by using CuK_α radiation ($\lambda = 1.540598 \text{ \AA}$) at room temperature in the angular range of $2\theta = 5\text{-}50^\circ$ with a scan step width of 0.02° and a fixed time of 0.2 s. The powder XRD patterns for the pure

powder sample of Compound **1** showed good agreement with the calculated XRD patterns from the single-crystal models (see Fig. S6).

Table S1. Summary of crystallographic data for compound **1**

Empirical formula	C ₉ H ₁₂ OF ₉ P	C ₉ H ₁₂ OF ₉ P
Formula weight	338.16	338.16
<i>T</i> , K	296(2)	363.15
Crystal system, space group	trigonal, <i>R3c</i>	trigonal, <i>R3c</i>
<i>a</i> , Å	15.3547(5)	15.5366(7)
<i>b</i> , Å	15.3547(5)	15.5366(7)
<i>c</i> , Å	10.0767(5)	10.1335(7)
γ , deg	120	120
<i>V</i> , Å ³	2057.46(17)	2118.4(2)
<i>Z</i>	6	6
<i>D</i> _{calc.} , g m ⁻³	1.638	1.590
μ , mm ⁻¹	0.297	0.288
<i>F</i> (000), e	1020	1021.8
θ range, deg	5.306→63.164	5.24→54.96
<i>hkl</i> range	-21 ≤ <i>h</i> ≤ 19 -18 ≤ <i>k</i> ≤ 20 -13 ≤ <i>l</i> ≤ 12	-21 ≤ <i>h</i> ≤ 22 -22 ≤ <i>k</i> ≤ 21 -13 ≤ <i>l</i> ≤ 14
Data/Restraints/parameters	1218 / 1 / 61	1082 / 1 / 61
Reflections collected/unique	5439 / 1218	8611 / 1082
<i>R</i> _{int}	0.0217	0.0567
Goodness-of-fit on <i>F</i> ²	1.011	1.004
<i>R</i> ₁ / <i>wR</i> ₂ [<i>I</i> > 2σ(<i>I</i>)]	0.0370 / 0.0964	0.0579 / 0.1613
<i>R</i> ₁ / <i>wR</i> ₂ (all data)	0.0401 / 0.0984	0.0666 / 0.1707
Largest peak and hole (e Å ⁻³)	0.31 / -0.22	0.64 / -0.26

Table S2. Selected bond lengths and angles of compound **1** at 296(2) K

Bond lengths	Å	Bond angles	deg
P(1)-O(1)	1.496(4)	O(1)-P(1)-C(1)	112.91(10)
P(1)-C(1)	1.803(3)	C(1) ^{#1} -P(1)-C(1) ^{#2}	105.82(12)
C(3)-F(1)	1.322(5)	F(1)-C(3)-F(2)	103.1(4)
C(3)-F(2)	1.324(6)	F(1)-C(3)-F(3)	105.3(3)
C(3)-F(3)	1.336(5)	F(2)-C(3)-F(3)	107.3(4)
C(1)-C(2)	1.515(4)	C(2)-C(1)-P(1)	112.1(2)
C(3)-C(2)	1.476(5)	C(3)-C(2)-C(1)	113.5(3)

Symmetry transformations used to generate equivalent atoms: ^{#1} -x + 2, -y + 1, -z; ^{#2} -x + 1, -y + 1, -z.

Table S3. Selected bond lengths and angles of compound **1** at 363.15 K

Bond lengths	Å	Bong angles	deg
P(1)-O(1)	1.488(5)	C(1)-P(1)-O(1)	112.56(14)
P(1)-C(1)	1.797(3)	C(1) ^{#1} -P(1)-C(1) ^{#2}	106.21(16)
F(1)-C(3)	1.298(7)	F(1)-C(3)-F(2)	106.0(5)
F(2)-C(3)	1.306(7)	F(1)-C(3)-F(3)	100.1(6)
F(3)-C(3)	1.343(8)	F(2)-C(3)-F(3)	105.7(5)
C(1)-C(2)	1.495(6)	C(2)-C(1)-P(1) ^{#2}	113.4(3)
C(2)-C(3)	1.454(7)	C(3)-C(2)-C(1)	116.3(4)

Symmetry transformations used to generate equivalent atoms: ^{#1} -x + 2, -y + 1, -z; ^{#2} -x + 1, -y + 1, -z.

Table S4. Summary of Nonlinear optical properties of different compounds.

Compound	Transmittance	Cut-off edge	Wavelength	References
NH ₄ B ₄ O ₆ F	<13%	156 nm	156-200 nm	1
KLi(HC ₃ N ₃ O ₃)·2H ₂ O	< 60%	237 nm	200-800 nm	2
NH ₄ Zn ₂ BO ₃ Cl ₂	< 60%	186 nm	190-300 nm	3
KZn ₂ BO ₃ Cl ₂	< 40%	193 nm	190-300 nm	3
RbZn ₂ BO ₃ Cl ₂	< 50%	198 nm	190-300 nm	3
KZn ₂ BO ₃ Br ₂	< 45%	206 nm	190-300 nm	3
Ca ₂ Na ₃ (CO ₃) ₃ F	< 40%	190 nm	190-300 nm	4
RbNaMgP ₂ O ₇	< 40%	185 nm	160-300 nm	5

NH ₄ NaLi ₂ (SO ₄) ₂	< 30%	< 186 nm	186-800 nm	6
NaZnCO ₃ (OH)	< 40%	201 nm	200-800 nm	7
NH ₄ Be ₂ BO ₃ F ₂	< 90%	153 nm	153-2000 nm	8
Ba ₃ P ₃ O ₁₀ Cl	< 85%	180 nm	200-2400 nm	9
Ba ₃ P ₃ O ₁₀ Br	< 90%	180 nm	200-2400 nm	9
PO(CH ₂ CH ₂ CF ₃) ₃	83%	< 200 nm	200-800 nm	Title compound

Table S5. The dipole moment vector of the whole unit at 296(2) K

method	dipole moment	Direction(x)	Direction(y)	Direction(z)
[0]	300.353191	0.863425	-0.498498	-0.077443
[1]	300.1664	0.863962	-0.498809	-0.068992
[2]	300.210696	0.863834	-0.498735	-0.071089
[3]	300.211525	0.863832	-0.498734	-0.071127
[4]	300.184253	0.86391	-0.498779	-0.069845
[5]	300.159156	0.863983	-0.498821	-0.068643

Table S6. The dipole moment vector of the whole unit at 363.15 K

method	dipole moment	Direction(x)	Direction(y)	Direction(z)
[0]	273.174779	-0.652788	0.376888	-0.657132
[1]	274.718535	-0.64912	0.37477	-0.66196
[2]	274.251033	-0.650227	0.375409	-0.66051
[3]	274.245909	-0.650239	0.375416	-0.660494
[4]	274.33628	-0.650025	0.375292	-0.660775
[5]	274.677038	-0.649218	0.374826	-0.661831

Table S7 Anisotropic Displacement Parameters ($\text{\AA}^2 \times 10^3$) for compound **1** at 296(2) K. The Anisotropic displacement factor exponent takes the form: $-2\pi^2[h^2a^{*2}U_{11}+2hka^*b^*U_{12}+\dots]$.

Atom	U ₁₁	U ₂₂	U ₃₃	U ₂₃	U ₁₃	U ₁₂
P1	32.0(3)	32.0(3)	28.1(4)	0	0	15.99(15)
C1	34.5(12)	41.0(14)	41.3(12)	-2.0(10)	-3.1(9)	21.1(11)
F1	132(3)	127(2)	78.9(17)	11.9(17)	-11.7(18)	99(2)
C3	71(2)	66(2)	71(2)	10.1(19)	7.9(19)	50(2)

O1	51.6(13)	51.6(13)	27.4(15)	0	0	25.8(6)
F2	67.1(17)	119(3)	196(4)	43(3)	35(2)	59.4(19)
C2	71(2)	69(2)	63(2)	-21.8(17)	-18.5(17)	52(2)
F3	145(3)	130(3)	108(3)	-19.5(16)	-9.1(17)	118(3)

Table S8 Anisotropic Displacement Parameters ($\text{\AA}^2 \times 10^3$) for compound **1** at 363.15 K. The Anisotropic displacement factor exponent takes the form: $-2\pi^2[h^2a^2U_{11}+2hka*b*U_{12}+\dots]$.

Atom	U_{11}	U_{22}	U_{33}	U_{23}	U_{13}	U_{12}
F3	185(5)	111(3)	299(7)	96(3)	-63(5)	-44(4)
P1	52.7(4)	52.7(4)	43.7(5)	26.3(2)	-0	0
O1	72.7(16)	72.7(16)	44.8(18)	36.4(8)	-0	0
F2	185(5)	226(7)	166(5)	175(6)	15(2)	8(3)
C1	68(2)	60.6(17)	62.0(15)	33.9(15)	2.4(14)	5.6(13)
C2	112(4)	102(3)	91(3)	76(3)	24(2)	22(2)
F1	232(5)	235(5)	117(3)	189(4)	-15(3)	19(3)
C3	106(4)	107(4)	105(3)	75(3)	-14(3)	-11(3)

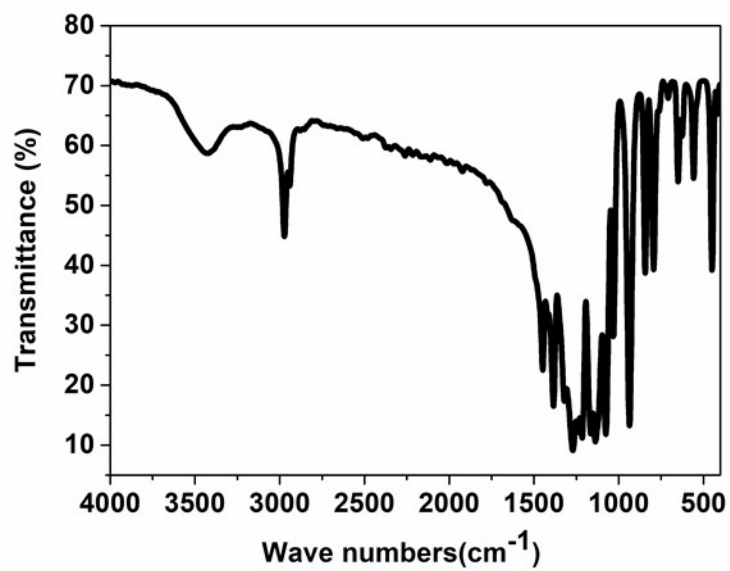


Fig.S1. Infrared spectrum of solid compound **1** in KBr pellets recorded at room temperature

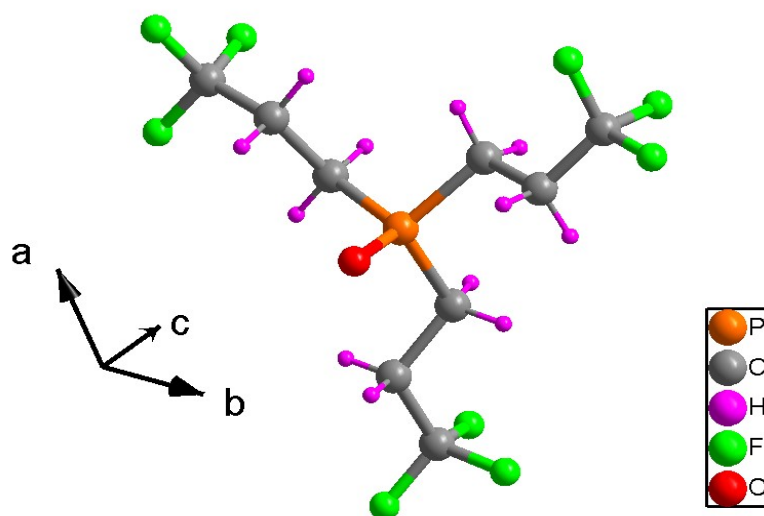


Fig. S2. Molecular structures of compound **1** at 296(2) K

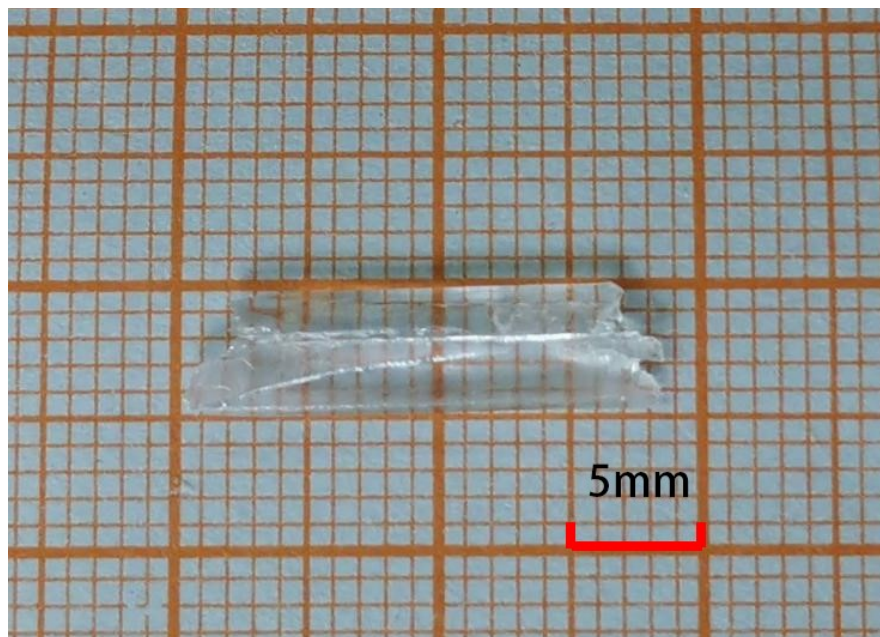
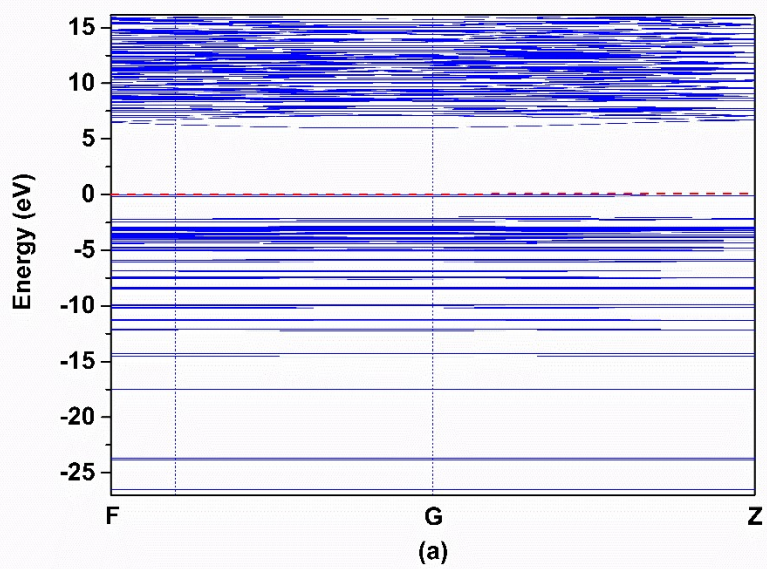


Fig. S3. Crystal size for compound **1**.



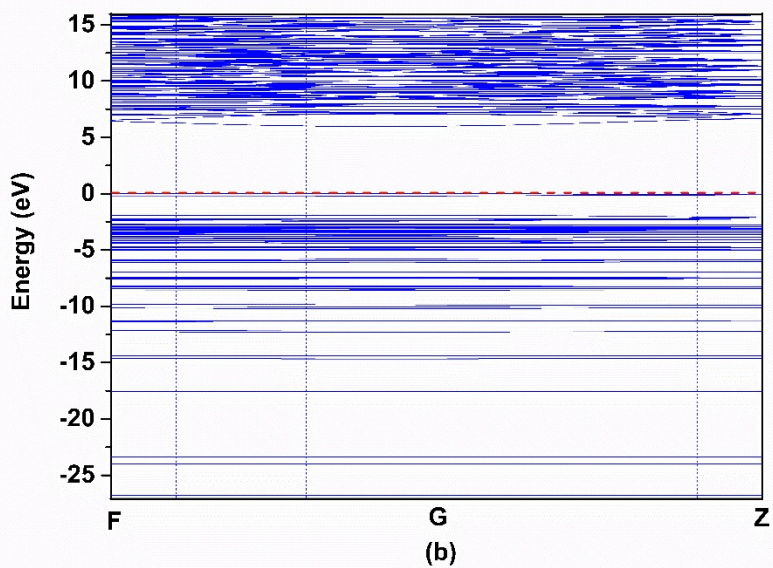


Fig. S4. Calculated electronic band structures for compound **1** in RTP (a) and in HTP (b).

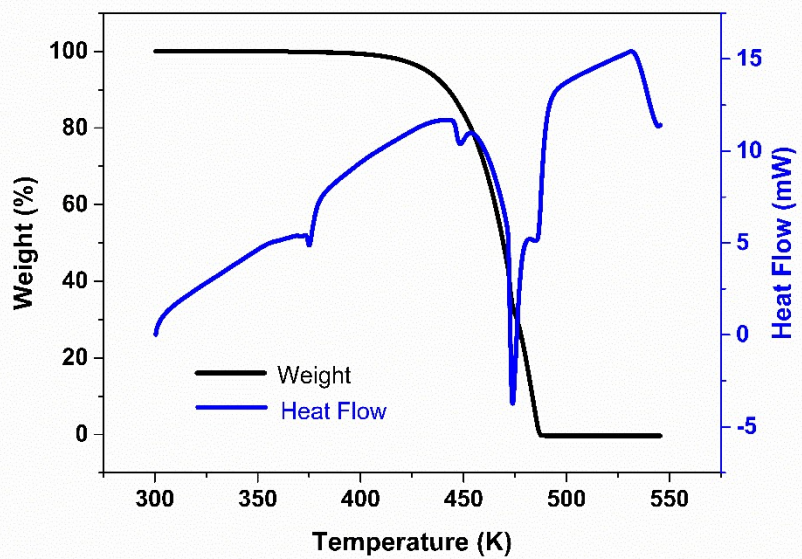


Fig.S5. Thermogravimetry-mass analysis for compound **1**.

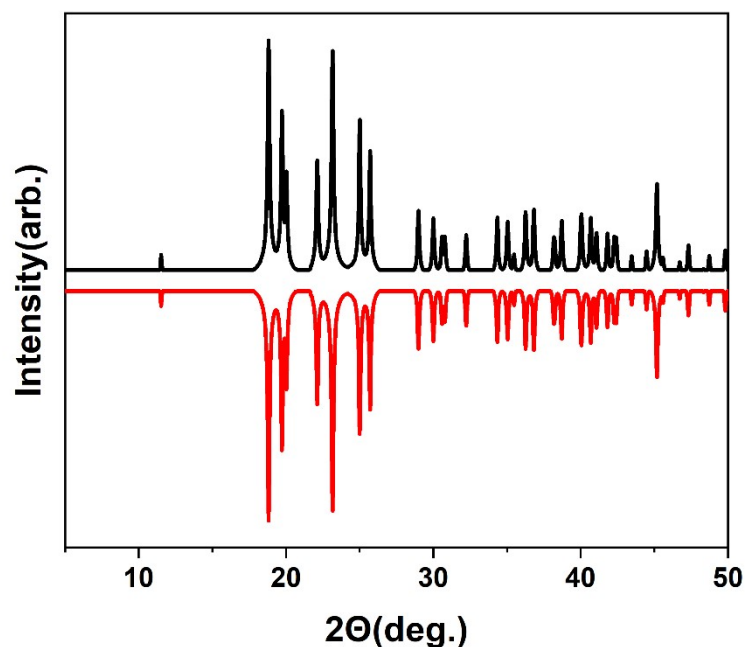


Fig. S6. The PXRD diagram for compound **1** at room temperature. The experimental data are in the black line and the simulated data are in the red line.

References:

- (1) Shi, G. Q.; Wang, Y.; Zhang, F. F.; Zhang, B. B.; Yang, Z. H.; Hou, X. L.; Pan S. L.; Kenneth R.; Poeppelmeier. *J. Am. Chem. Soc.* **017**, 139, 10645.
- (2) Lin, D. H.; Luo, M.; Lin, C.S.; Xu, F.; Ye, N. *J. Am. Chem. Soc.* **019**, 141, 3390.
- (3) Yang, G. S.; Gong, P. F.; Lin, Z. S.; Ye, N. *Chem. Mater.* **2016**, 28, 9122.
- (4) Luo, M.; Song, Y. X.; Lin, C. S.; Ye, N.; Cheng, W. D.; Long, X. F. *Chem. Mater.* **2016**, 28, 2301.
- (5) Zhao, S. G.; Yang, X. Y.; Yang, Y.; Kuang, X. J.; Lu, F. Q.; Shan, P.; Sun, Z. H.; Lin, Z. S.; Hong, M. C.; Luo, J. H. *J. Am. Chem. Soc.* **2018**, 140, 1592.
- (6) Li, Y. Q.; Liang, F.; Zhao, S. G.; Li, L. N.; Wu, Z. Y.; Ding, Q.R.; Liu, S.; Lin, Z. S.; Hong, M. C.; Luo, J. H. *J. Am. Chem. Soc.* **2019**, 141, 3833.
- (7) Peng, G.; Lin C. S.; Ye, N. *J. Am. Chem. Soc.* **2020**, 142, 20542.
- (8) Peng, G.; Ye, N.; Lin, Z. S.; Kang, L.; Pan, S. L.; Zhang, M.; Lin, C. S.; Long, X. F.; Luo, M.; Chen, Y.; Tang, Y. H.; Xu, F.; Yan, T. *Angew. Chem. Int. Ed.* **2018**, 57, 8968.
- (9) Yu, P.; Wu, L. M.; Zhou, L. J.; Chen, L. *J. Am. Chem. Soc.* **2014**, 136, 480.
- (10) Lu, T.; Chen, F. W. *J. Comput. Chem.* **2012**, 33, 580.
- (11) Humphrey, W.; Dalke, A.; Schulten, K. *J. Molec. Graphics*, **1996**, 14.1, 33.
- (12) Frisch, M. J.; Trucks, G. W.; Schlegel, H. B.; Scuseria, G. E.; Robb, M. A.; Cheeseman, J. Scalmani, R.; G.; Barone, V.; Petersson, G. A.; Nakatsuji, H.; Li, X.; Caricato, M.; Marenich, A.; Bloino, J.; Janesko, B. G.; Gomperts, R.; Mennucci, B.; Hratchian, H. P.; Ortiz, J. V.; Izmaylov, A. F.; Sonnenberg, J. L.; Williams-Young D.; Ding, F.; Lipparini, F.; Egidi, F.; Goings, J.; Peng, B.; Petrone, A.; Henderson, T.; Ranasinghe, D.; Zakrzewski, V. G.; Gao, J.; Rega, N.; Zheng G.; Liang, W.; Hada, M.; Ehara, M.; Toyota, K.; Fukuda, R.; Hasegawa, J.; Ishida, M.; Nakajima, T.; Honda, Y.; Kitao, O.; Nakai, H.; Vreven, T.; Throssell, K.; Montgomery, J. A.; Peralta, J. E.; Ogliaro, F.;

Bearpark, M.; Heyd, J. J.; Brothers, E.; Kudin, K. N.; Staroverov, V. N.; Keith, T.; Kobayashi, R.; Normand, J.; Raghavachari, K.; Rendell, A.; Burant, J. C.; Iyengar, S. S.; Tomasi, J.; Cossi, M.; Millam, J. M.; Klene, M.; Adamo, C.; Cammi, R.; Ochterski, J. W.; Martin, R. L.; Morokuma, K.; Farkas, O.; Foresman, J. B.; Fox, D. J.; Gaussian, 09; Revision A.02, Gaussian, Inc., Wallingford CT, **2016**.